

# Design of Experiment-based Optimization of Dual Drug-loaded Liquid Crystalline Nanoparticles Containing 5-Fluorouracil and Melatonin

Karthikeyan Sathasivam, Subramanian Somaskanthan, S. M. Habibur Rahman

Department of Pharmaceutics, PSG College of Pharmacy (Affiliated to the Tamil Nadu Dr. MGR Medical University, Chennai), Coimbatore, Tamil Nadu, India

## Abstract

**Introduction:** Combination chemotherapy offers improved therapeutic outcomes by targeting multiple oncogenic pathways simultaneously; however, co-delivery of drugs with contrasting physicochemical properties remains a major formulation challenge. Liquid crystalline nanoparticles (LCNs) possess a unique bicontinuous cubic architecture capable of encapsulating both hydrophilic and lipophilic agents within a single nanostructure. The present study aimed to develop and optimize dual drug-loaded LCNs for the co-delivery of 5-fluorouracil (5-FU) and melatonin (MEL) using a design of experiments-based approach. **Materials and Methods:** LCNs were prepared by a top-down homogenization method employing glyceryl monooleate (GMO) and Poloxamer 407. A three-factor Box–Behnken design was applied to evaluate the influence of GMO concentration, stabilizer concentration, and homogenization speed on particle size, zeta potential, and entrapment efficiency. Characterization of the optimized formulation was characterized by dynamic light scattering, X-ray diffraction (XRD), Field emission scanning electron microscopy (FESEM), and *in vitro* drug release studies. **Results and Discussion:** Particle size ranged from 102nm to 384.7nm, and statistical modeling confirmed significant effects of lipid concentration and homogenization speed. The optimized formulation exhibited a particle size of 187.8 nm, zeta potential of  $-35.9$  mV, and entrapment efficiencies of 82.62% for 5-FU and 86.52% for MEL. XRD analysis revealed amorphous drug incorporation, while FESEM confirmed nanoscale morphology. *In vitro* release studies demonstrated rapid release of pure drugs, whereas LCNs exhibited a biphasic sustained release pattern extending up to 8 h. **Conclusion:** The optimized LCNs system successfully enabled stable co-encapsulation and sustained release of hydrophilic and lipophilic drugs, indicating its potential as a promising platform for synergistic anticancer therapy.

**Key words:** 5-Fluorouracil, box-behnken design, liquid crystallin nanoparticles, melatonin

## INTRODUCTION

Combination therapy has become a cornerstone of contemporary cancer treatment because it allows multiple cellular pathways to be targeted simultaneously, improves therapeutic outcomes, and helps delay the emergence of drug resistance.<sup>[1]</sup> Despite these advantages, the effectiveness of many combination regimens is limited by practical pharmaceutical challenges, particularly when the drugs involved differ substantially in their physicochemical properties.<sup>[2]</sup> Hydrophilic and hydrophobic agents often display contrasting solubility, stability, absorption, tissue distribution, and elimination behaviors. As a result, they rarely reach the target site in optimal proportions or at the same time, which can

reduce their synergistic potential and lead to variable clinical responses. These challenges highlight the need for advanced drug delivery systems capable of co-encapsulating dissimilar molecules, releasing them in a coordinated manner, and ensuring their synchronized action at the cellular level.<sup>[3]</sup>

In recent years, nanotechnology-based delivery systems have emerged as promising tools to address these

### Address for correspondence:

Subramanian Somaskanthan, Department of Pharmaceutics, PSG College of Pharmacy, Coimbatore, Tamil Nadu, India.  
E-mail: subbu3j@gmail.com

**Received:** 26-02-2026

**Revised:** 23-03-2026

**Accepted:** 31-03-2026

limitations.<sup>[4]</sup> Among them, liquid crystalline nanoparticles (LCNs), commonly known as LCNs, have gained considerable attention due to their distinctive internal structure and exceptional versatility.<sup>[5]</sup> LCNs are nanoscale dispersions of bicontinuous cubic liquid crystalline phases formed by amphiphilic lipids in aqueous environments. Their three-dimensional architecture comprises a continuous lipid bilayer arranged into a highly ordered periodic structure, separating two intertwined but non-intersecting aqueous channel networks. This unusual organization creates separate yet interconnected domains, allowing both hydrophilic and hydrophobic molecules to be accommodated within a single carrier system.<sup>[6]</sup> The presence of aqueous nanochannels enables efficient loading of water-soluble drugs, while the lipid bilayer region provides a suitable environment for lipophilic compounds.<sup>[7]</sup> LCNs also provide sustained and controlled drug release, which helps to avoid burst effects, reduces peak-related toxicity, and maintains therapeutically relevant drug concentrations over extended periods.

In the present study, the dual-drug loading capability of LCNs is investigated using 5-Fluorouracil (5-FU), a hydrophilic chemotherapeutic agent, and Melatonin (MEL), a hydrophobic bioactive molecule known for its antioxidant, immunomodulatory, and chemosensitizing effects. MEL in contrast, has been shown to enhance the anticancer activity of chemotherapeutic drugs while simultaneously protecting normal tissues from oxidative and inflammatory damage.<sup>[8,9]</sup> However, its poor aqueous solubility, short biological half-life, and extensive first-pass metabolism limit its therapeutic use. The primary aim of this research is to develop, optimize, and evaluate dual-drug-loaded LCNs for the concurrent delivery of 5-FU and a MEL. By integrating experimental design with advanced nanocarrier engineering, this work seeks to enhance controlled release, thereby improve bioavailability, minimize systemic toxicity.

## MATERIALS AND METHODS

5-FU and MEL were obtained from TCI Chemicals. Glycerol monooleate (GMO) was a kind gift from Mohini Organic's Private Limited, Mumbai, India. Poloxamer 407 was obtained from Sigma Aldrich. All the other chemicals and reagents used were of analytical grade.

### Formulation of 5-FU and MEL co-loaded LCNs

LCNs co-loaded with 5-FU and MEL were prepared using a top-down approach.<sup>[10]</sup> MEL, being hydrophobic, was incorporated into the lipid phase by dissolving it in molten GMO containing Poloxamer 407 as a stabilizer at approximately 70°C. In parallel, 5-FU was dissolved in the aqueous phase under continuous stirring at the same temperature to maintain phase compatibility and prevent

premature lipid solidification. The aqueous phase was then added slowly, dropwise, to the molten lipid phase under constant mechanical stirring to form a coarse dispersion. The resulting dispersion was subsequently subjected to high-shear homogenization using a high-speed homogenizer. Following homogenization, the formulations were allowed to equilibrate at room temperature to enable complete self-assembly of the LCNs architecture.

### Box Behnken design-based optimization of dual drug-loaded LCNs formulation

The LCNs formulation was optimized using a Box–Behnken design using Design-Expert® software (version 13). A three-factor experimental design with five replicates at the center point was selected to systematically evaluate the influence of formulation and process variables on critical quality attributes. GMO (X1) and Poloxamer 407 (X2) were chosen as the key formulation variables, while homogenization speed (X3) was included as the primary process parameter. Particle size (Y1), zeta potential (Y2), and entrapment efficiency (EE) (Y3) were identified as the dependent responses, as they are critical indicators of formulation performance and stability. The working ranges and levels for GMO are 1–5%w/w, Poloxamer 407 is 0.5–3%w/w, and homogenization speed is 10,000–20,000 rpm. Using these inputs, the software generated 17 experimental runs, which are presented in Table 1. The responses were evaluated with the objective of minimizing particle size, maintaining zeta potential within an acceptable range, and maximizing EE.

### Analysis of particle size and zeta potential

Particle size, polydispersity index, and zeta potential of all prepared formulations were measured using a Zetasizer Nano ZS 90 (Malvern Instruments, UK). Zeta potential measurements were carried out at 25°C using a dip cell electrode.

### Measurement of EE

EE of the prepared formulations was determined using an ultracentrifugation method. The amounts of free 5-FU and MEL were quantified using ultraviolet spectrophotometry at 265 nm and 277 nm, respectively.<sup>[11]</sup>

### X-ray diffraction (XRD) spectroscopy

XRD analysis was carried out to assess the crystalline characteristics of LCNs co-loaded with 5-FU and MEL using an Empyrean diffractometer (Malvern Panalytical). Samples were scanned over a 2θ range of 0–80° at a scanning rate of 10°/min to evaluate the physical state of the incorporated drugs within the LCNs matrix.

**Table 1: Box Behnken design of optimization of liquid crystalline nanoparticles**

Run	GMO % w/w	P-407% w/w	Homogenization speed (rpm)	Particle size (nm)	Zeta potential (mV)	EE of 5-fluorouracil %	EE melatonin %
1	1	0.5	15000	178.6	-25.8	57.75	81
2	5	0.5	15000	299.1	-41.9	71.85	84.8
3	1	3	15000	143.5	-20.9	64.55	87.8
4	5	3	15000	260	-24.54	72.15	85
5	1	1.75	10000	232.1	-18.71	65.45	76
6	5	1.75	10000	384.7	-25.2	73.95	84
7	1	1.75	20000	143	-19.1	55.95	86
8	5	1.75	20000	283	-24.8	67.85	78.3
9	3	0.5	10000	211	-37.1	78.00	82.1
10	3	3	10000	238.3	-19.8	78.75	86
11	3	0.5	20000	164.8	-33.7	73.40	82.5
12	3	3	20000	102	-27.1	76.65	87.5
13	3	1.75	15000	157	-24.8	87.6	88.5
14	3	1.75	15000	167.8	-25	82.15	88.7
15	3	1.75	15000	154.4	-32.3	83.05	87.5
16	3	1.75	15000	171	-24.8	85.94	89
17	3	1.75	15000	164.5	-27.9	84.89	89

GMO: Glyceryl monooleate, P407: Poloxamer 407, EE: Entrapment efficiency

### Field emission-scanning electron microscopy (FE-SEM)

The surface morphology of 5-FU and MEL co-loaded LCNs was examined using FE-SEM.

### *In vitro* release study

*In vitro* release of 5-FU and MEL from the co-loaded LCNs was evaluated using the dialysis bag diffusion method. The dialysis bag was immersed in 250 mL of (phosphate-buffered saline, pH 7.4) and maintained under constant stirring at 100 rpm using a magnetic stirrer. At predetermined time intervals, a fixed volume of the release medium was withdrawn for analysis and immediately replaced with an equal volume of fresh buffer to maintain sink conditions.

## RESULTS AND DISCUSSION

### Preparation of LCNs by top-down technique

The Box Behnken-based design of optimization of LCNs co-loaded with 5-FU and MEL results in 17 runs, and the results are listed in Table 1.

### Effect of variables on particle size

The particle size of the dual drug-loaded LCNs ranged from 102 to 384.7 nm across the experimental design space.

Statistical analysis revealed that a quadratic model best described the relationship between the formulation variables and particle size [Table 2 and Figure 1a]. The model was found to be robust and reliable, as indicated by a non-significant lack of fit. The high Model F-value (80.51) further confirmed the statistical significance of the model ( $P < 0.05$ ). The final polynomial equation describing the effect of the independent variables on particle size was:

$$\text{Particle size} = 162.94 + 66.20A - 13.71B - 46.66C - 1.00AB - 3.15AC - 22.53BC + 69.52A^2 - 12.16B^2 + 28.24C^2$$

Where A represents GMO concentration, B represents Poloxamer 407 concentration, and C denotes homogenization speed. Among the studied factors, GMO (factor A) and homogenization speed (factor C) exerted the most pronounced influence on particle size. An increase in GMO concentration resulted in a significant increase in particle size, which can be attributed to the higher lipid content increasing the viscosity of the dispersed phase and promoting the formation of larger aggregates. This observation is consistent with previous reports describing the role of lipid viscosity in controlling nanostructure dimensions.<sup>[12]</sup> In contrast, homogenization speed exhibited a strong negative effect on particle size (coefficient -46.66), indicating that higher shear forces facilitated finer dispersion and reduced particle dimensions.<sup>[13]</sup>

### Effect of variables on zeta potential

Zeta potential is a key indicator of colloidal stability, reflecting the magnitude of electrostatic repulsion between

**Table 2:** Analysis of variance results for response 1: Particle size

Source	Sum of squares	df	Mean square	F-value	P-value
Model	80892.78	9	8988.09	80.51	<0.0001 <sup>S</sup>
A-GMO	35059.52	1	35059.52	314.04	<0.0001
B-P 407	1504.26	1	1504.26	13.47	0.0080
C-Homogenization speed	17419.11	1	17419.11	156.03	<0.0001
AB	4.00	1	4.00	0.0358	0.8552
AC	39.69	1	39.69	0.3555	0.5698
BC	2029.50	1	2029.50	18.18	0.0037
Residual	781.47	7	111.64		
Lack of fit	582.24	3	194.08	3.90	0.1110 <sup>NS</sup>

df: Degree of freedom, GMO: Glyceryl Monooleate, P407: Poloxamer 407, S: Significant, NS: Not significant

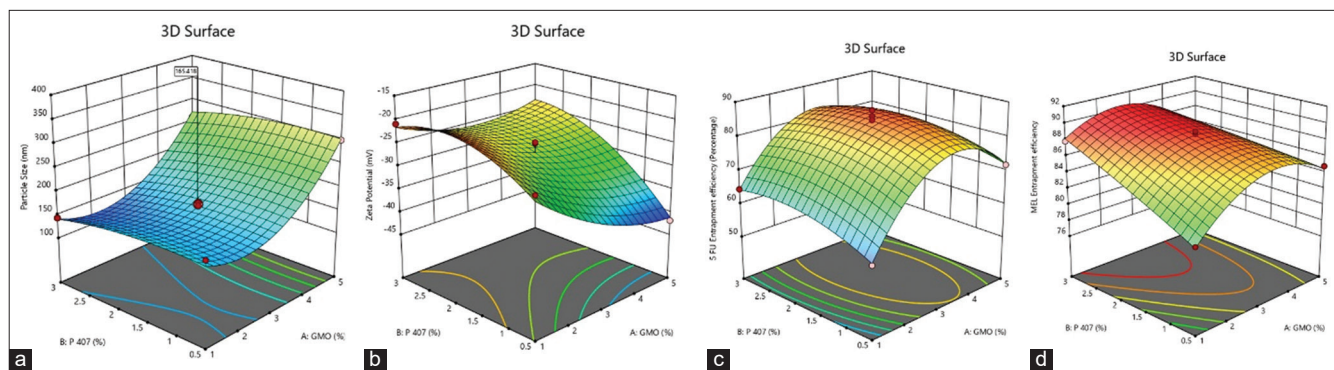


**Figure 1:** 3D response surface plot of each response: (a) Particle size, (b) zeta potential, (c) 5-fluorouracil entrapment efficiency (EE), (d) melatonin EE

particles and their resistance to aggregation. In this study, the zeta potential of the dual drug-loaded LCNs ranged from  $-18.7$  mV to  $-41.9$  mV, suggesting the formation of moderately to highly stable nanoparticles. Figure 1b presents the three-dimensional response surface illustrating the combined effects of formulation and process variables on the zeta potential of the dual drug-loaded LCNs. The model was statistically significant ( $F = 8.89$ ,  $P = 0.0044$ ), with a non-significant lack of fit ( $F = 0.29$ ,  $P = 0.8291$ ), confirming that it appropriately represented the experimental data. The relationship between the independent variables and zeta potential [Table 3] was expressed by the polynomial equation:

$$\text{Zeta potential} = -26.96 - 3.99A + 5.77B - 0.49C + 3.12AB + 0.20AC - 2.68BC + 3.07A^2 - 4.40B^2 + 1.93C^2$$

Among the linear terms, GMO (A) and Poloxamer 407 (B) showed statistically significant effects on zeta potential ( $P < 0.05$ ). The negative coefficient of GMO ( $-3.99$ ) indicates that increasing lipid concentration reduced the magnitude of zeta potential, likely due to masking of surface charges by the lipid matrix and reduced exposure of ionizable groups at the particle interface. This behavior has been reported for lipid-based nanocarriers, where increased lipid content alters interfacial charge distribution. In contrast, Poloxamer 407 exerted a strong positive effect ( $+5.77$ ), suggesting that higher stabilizer

concentrations enhanced surface charge magnitude through improved surface coverage and interfacial stabilization.<sup>[14]</sup>

### Effect of variables on EE%

EE is a critical parameter that reflects the ability of the LCNs nanostructure to incorporate and retain drug molecules within its internal architecture. In the present study, the entrapment behaviors of 5-FU [Figure 1c], a hydrophilic drug, and MEL [Figure 1d], a water-insoluble drug, showed distinct trends across the experimental domain. The polynomial equation in coded terms was:

$$\text{5-FU EE} = 84.68 + 5.26A + 1.38B - 2.79C - 1.63AB + 0.85AC + 0.63BC - 14.54A^2 - 3.62B^2 - 4.39C^2$$

Among the linear terms, GMO (A) concentration and homogenization speed (C) exerted statistically significant effects on 5-FU entrapment, whereas the linear contribution of Poloxamer 407 was not significant. The positive coefficient of GMO indicates that increasing lipid concentration initially enhanced 5-FU retention, likely due to the formation of a more organized bicontinuous cubic phase with tortuous aqueous channels capable of physically confining the hydrophilic drug. However, the strongly negative quadratic term of GMO suggests

**Table 3:** Analysis of variance (ANOVA) results for response 2: Zeta potential

Source	Sum of squares	df	Mean square	F-value	P-value
Model	593.50	9	65.94	8.89	0.0044 <sup>S</sup>
A-GMO	127.44	1	127.44	17.17	0.0043
B-P 407	266.34	1	266.34	35.89	0.0005
C-Homogenization speed	1.89	1	1.89	0.2549	0.6291
AB	38.81	1	38.81	5.23	0.0561
AC	0.1560	1	0.1560	0.0210	0.8888
BC	28.62	1	28.62	3.86	0.0903
Residual	51.94	7	7.42		
Lack of Fit	9.37	3	3.12	0.2935	0.8291 <sup>NS</sup>

df: Degree of freedom, GMO: Glyceryl monooleate, P407: Poloxamer 407, S: Significant, NS: Not significant

**Table 4:** Optimization and validation of liquid crystalline nanoparticles

Solution 1 of 16 response	Predicted mean	Observed	Standard deviation	95% PI low	95% PI high
Particle size (nm)	181.172	187.8	10.5659	151.941	210.40
Zeta potential (mV)	-38.4847	-35.9	2.72409	-46.021	-30.94
5-fluorouracil EE (%)	80.7166	82.62	2.10104	74.904	86.52
Melatonin EE (%)	86.5256	87.13	0.628433	84.7871	88.26

EE: Entrapment efficiency, PI: Prediction interval

that excessive lipid content leads to structural saturation or phase reorganization, thereby reducing the effective aqueous domain volume and promoting drug loss. Homogenization speed exhibited a negative linear effect, implying that excessive mechanical energy may facilitate drug diffusion into the external aqueous phase during particle formation. In contrast, MEL entrapment followed a different trend. The corresponding polynomial equation in coded terms was:

$$\text{MEL EE} = 88.54 + 0.16A + 1.99B + 0.78C - 1.65AB - 3.93AC + 0.28BC - 3.67A^2 - 0.22B^2 - 3.80C^2$$

Here, poloxamer 407 (B) and homogenization speed (C) showed statistically significant linear effects, whereas GMO did not. The positive coefficient of Poloxamer 407 indicates that increasing stabilizer concentration enhanced MEL entrapment, likely by improving interfacial stabilization and limiting drug diffusion into the external aqueous phase. This behavior is particularly relevant for hydrophobic drugs, which rely on strong lipid-drug interactions for retention within the bilayer. Moderate increases in homogenization speed also improved MEL entrapment, possibly due to rapid particle formation and uniform encapsulation.<sup>[15]</sup> However, the significant quadratic term of homogenization speed suggests that excessive mechanical energy disrupts the internal nanostructure and promotes drug loss.

### Selection of the optimized batch

Numerical optimization was performed using a desirability function approach to simultaneously achieve minimal

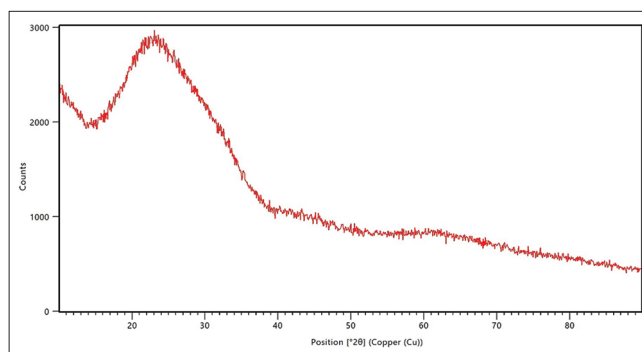


**Figure 2:** Characterization of optimized batch: X-ray crystallography graph

particle size, sufficiently high zeta potential magnitude, and maximum entrapment efficiencies for both 5-FU and MEL. A total of 16 feasible solutions were generated within the experimental design space; among these, the formulation comprising approximately 3.36% GMO, 0.50% Poloxamer 407, and a homogenization speed of 14,544 rpm was identified as the optimal batch [Table 4], as it exhibited the highest overall desirability value (0.7898).

Two-sided confidence = 95%

### Characterization of optimized batch: X-ray crystallography graph and FE-SEM

The XRD graph of LCNs revealed amorphous profile [Figure 2] characterized by a broad diffuse Bragg peak, and absence of characteristic sharp peaks of 5-FU and MEL.

This confirms successful drug entrapment inside LCN. The FE-SEM image of the freeze-dried LCN exhibited the presence of nanosized particles with relatively uniform morphology, and there is no evidence of excessively large aggregates.

### ***In vitro* drug release of pure 5-FU and optimized 5-FU-loaded LCNs**

The *in vitro* release study revealed rapid diffusion of pure 5-FU, achieving complete release within 1 h, consistent with membrane diffusion-controlled kinetics. LCNs release extended to 94.72% over 8 h. The prolonged release behavior is attributed to the diffusion of 5-FU through the lipid matrix. These findings confirm effective encapsulation and sustained drug delivery from the LCNs system.

### ***In vitro* drug release of pure MEL and optimized MEL-loaded LCNs**

The *in vitro* release study revealed rapid diffusion of pure MEL, achieving complete release within 1 h. In contrast, the LCNs formulation exhibited a biphasic release profile characterized by a reduced initial burst (21.24% at 1 h) followed by a sustained diffusion-controlled phase, reaching 81.90% at 8 h. The prolonged release behavior confirms effective encapsulation and sustained release capability.

### **Release kinetics**

The release kinetics indicated Higuchi-type release behavior suggesting diffusion-controlled release of 5-FU and MEL. This confirms dual drug incorporated LCNs exhibited sustained release.

## **CONCLUSION**

Design of experiment-based optimization of dual drug-loaded LCNs for the co-delivery of 5-FU and MEL was successfully developed and optimized. From the results, it is evident that among the variables studied, GMO and homogenization speed has high influence on particle size, whereas stabilizer concentration has influenced zeta potential and entrapment of MEL. Encapsulation efficiency showed that both hydrophilic and lipophilic drugs successfully encapsulated in LCN. Characterization by XRD confirmed amorphous drug incorporation, and FE-SEM confirmed the nanoparticle morphology. The *in vitro* release profile indicated that there is a sustained release of dual drug-loaded LCN compared to pure drug, and the release kinetics analysis indicated Higuchi model diffusion-controlled release from LCNs. These findings conclude LCNs formulation warranting nanosized, dual drug delivery capable of sustained release, making it a suitable candidate for synergistic anticancer therapy.

## **ACKNOWLEDGMENTS**

This work received financial assistance from the PSG PRIME grant (Project code: PSGCP/B2025/01) sponsored by PSG Institute of Medical Science and Research. This work is an integral part of Ph.D research program registered under The Tamil Nadu Dr. M.G.R. Medical University, Chennai. We thank PSG College of Pharmacy, Coimbatore, for providing all the facilities and support.

## **REFERENCES**

1. Bayat Mokhtari R, Homayouni TS, Baluch N, Morgatskaya E, Kumar S, Das B, *et al.* Combination therapy in combating cancer. *Oncotarget* 2017;8:38022-43.
2. Singh H, Balusamy SR, Sukweenadhi J, Shrivastav A, Mohanprasanth A, Saravanan M, *et al.* Engineering combination nanomedicines to overcome cancer resistance. *RSC Adv* 2026;16:5128-67.
3. Subash P, Khute S. Recent advances in lyotropic liquid crystal nanoparticle formulations for drug delivery systems. *Front Soft Matter* 2025;5:1658466.
4. Li X, Peng X, Zoulikha M, Boafu GF, Magar KT, Ju Y, *et al.* Multifunctional nanoparticle-mediated combining therapy for human diseases. *Signal Transduct Target Ther* 2024;9:1.
5. Badiger P, Mannur VS, Koli R. Dual drug-loaded cubosome nanoparticles for hepatocellular carcinoma: A design of experiment approach for optimization and *in vitro* evaluation. *Future J Pharm Sci* 2024;10:38.
6. Sivadasan D, Sultan MH, Alqahtani SS, Javed S. Cubosomes in drug delivery-a comprehensive review on its structural components, preparation techniques and therapeutic applications. *Biomedicines* 2023;11:1114.
7. Zeng L, Ke Y, Zheng C, Song H, Liu Z, Hu X, *et al.* Remote loading of hydrophilic drug into cubosomes by transmembrane pH-gradient and characterization of drug-loaded cubosomes prepared by different method. *J Pharm Sci* 2023;112:1119-29.
8. Pan S, Guo Y, Hong F, Xu P, Zhai Y. Therapeutic potential of melatonin in colorectal cancer: Focus on lipid metabolism and gut microbiota. *Biochim Biophys Acta Mol Basis Dis* 2022;1868:166281.
9. Cao Y, Zhang H, Chen X, Li C, Chen J. Melatonin: A natural guardian in cancer treatment. *Front Pharmacol* 2025;16:1617508.
10. Umar H, Wahab HA, Gazzali AM, Tahir H, Ahmad W. Cubosomes: Design, development, and tumor-targeted drug delivery applications. *Polymers (Basel)* 2022;14:3118.
11. Zaki RM, Alkharashi LA, Sarhan OM, Almurshedi AS, Aldosari BN, Said M. Box-Behnken optimization of cubosomes for enhancing the anticancer activity of metformin: Design, characterization, and *in-vitro* cell proliferation assay on MDA-MB-231 breast and LOVO

- colon cancer cell lines. *Int J Pharm X* 2023;6:100208.
12. Mathew M, Patil A, Hemanth G. Development and characterization of sulfasalazine cubosomes for potential transdermal drug delivery. *Pharm Nanotechnol* 2025;13:320-7.
  13. Bei D, Marszalek J, Youan BB. Formulation of dacarbazine-loaded cubosomes--Part II: Influence of process parameters. *AAPS PharmSciTech* 2009;10:1040.
  14. Kojarunchitt T, Hook S, Rizwan S, Rades T, Baldursdottir S. Development and characterisation of modified poloxamer 407 thermoresponsive depot systems containing cubosomes. *Int J Pharm* 2011;408:20-6.
  15. Lai J, Chen J, Lu Y, Sun J, Hu F, Yin Z, *et al.* Glyceryl monooleate/poloxamer 407 cubic nanoparticles as oral drug delivery systems: I. *In vitro* evaluation and enhanced oral bioavailability of the poorly water-soluble drug simvastatin. *AAPS PharmSciTech* 2009;10:960-6.

**Source of Support:** Nil. **Conflicts of Interest:** None declared.